Journal of Chemical Metrology
www.acgpubs.org
Open Access
This article is licensed under CC-BY-NC-ND 4.0
ORIGINAL ARTICLE

Polymeric particle-contact effects on apparent phenylalanine recovery by an enzymatic colorimetric assay

Gülsüm Çiçek[1,2], Hasan Saygin[3], Mustafa Özyürek[1] and Asli Baysal[4*]

[1]İstanbul University-Cerrahpaşa, Engineering Faculty, Department of Chemistry, Division of Analytical Chemistry, Istanbul, Türkiye
[2]Istanbul Gedik University, Vocational School, Chemical Technology Programme, Istanbul, Türkiye
[3]Istanbul Aydin University, Application and Research Center for Advanced Studies, Istanbul, Türkiye
[4]Istanbul Technical University, Department of Chemistry, Faculty of Science and Letters, Istanbul, Türkiye

Cite This: *J. Chem. Metrol.* 2026, 20(2), e26104051

Read Online

Abstract: Contact with polymeric particulate materials may change the response of enzymatic colorimetric assays through analyte partitioning, filtration losses, or matrix-dependent effects. This study examined apparent phenylalanine (Phe) signal recovery following contact with particles derived from polyethylene terephthalate (PET) bottles, polypropylene (PP) plates, and cellulose-based paper cups. Materials were characterized by FTIR and Raman spectroscopy and contacted with buffered Phe solutions (20, 60, or 100 µm) at particle loadings of 1, 3, or 10 mg/mL for nominal durations of 2, 6, 24, 48, and 96 h. After 0.45-µm filtration, filtrates were analyzed by an enzyme/developer-based assay at 450 nm. Apparent signal recovery was normalized to concentration- and time-matched Phe-only controls. Across 45 conditions per material, mean apparent recoveries were 70.5% for PET (range 40.3–91.2%), 41.9% for PP (7.1–85.9%), and 7.3% for cellulose-based particles (0.2–24.6%). PET showed a loading-associated decline in recovery, whereas PP exhibited more variable, nonmonotonic profiles. The pronounced suppression observed for cup-derived material showed that effects were not confined to synthetic plastic particles. Because measurements were made on processed filtrates, reduced colorimetric response cannot be assigned uniquely to Phe adsorption. Potential contributions include particle-associated analyte removal, soluble matrix constituents, and filter-passing particulate matter. These findings identify substantial material-dependent changes in the apparent Phe analytical response under controlled buffer conditions and support the use of matrix-matched and orthogonal measurements to distinguish analyte depletion from assay interference.

Keywords: Phenylalanine, polymeric particles, enzymatic colorimetric assay, assay interference

1 Introduction

Phenylalanine (Phe) is an essential aromatic amino acid involved in protein biosynthesis and in metabolic pathways that support tyrosine and catecholamine production. Its concentration is of particular clinical relevance in phenylketonuria (PKU), where deficient phenylalanine hydroxylase activity impairs Phe metabolism and necessitates accurate and sustained biochemical monitoring. Quantification is therefore important not only in metabolic research but also in neonatal screening and follow-up of patients with PKU (Waisbren et al., 2007; Sebastião et al., 2020; Pinto et al., 2023).

Chromatographic and mass-spectrometric methods can provide selective Phe measurements in complex biological matrices, whereas enzymatic colorimetric methods offer practical advantages in throughput, accessibility, and operational simplicity. Enzyme-coupled assays ultimately convert the analyte-dependent biochemical reaction into an optical readout. Consequently, accuracy depends on more than the chemical presence of Phe: enzyme function, developer chemistry, sample composition, light transmission, and the recovery of soluble analyte after sample processing can all contribute to the measured absorbance. Signal loss should therefore not automatically be interpreted as analyte depletion (Rudy et al., 1987; Schulze et al., 2002; De Silva et al., 2010; Peat & Garg, 2016).

Global plastics production reached 430.9 million tonnes in 2024, with polypropylene (PP) and polyethylene terephthalate (PET) accounting for 19.0% and 6.2% of the reported

*Corresponding Author: Asli Baysal. Email: baysalas@itu.edu.tr
Received: October 23, 2026
Revised: November 16, 2026
Accepted: November 17, 2026
Published: November 26, 2026

Copyright © 2026. Published by ACG Publications.

total, respectively (PlasticsEurope, 2025). For 2019, the OECD estimated global plastics use at 460 million tonnes, including 73 million tonnes of PP and 25 million tonnes of PET (OECD, 2022). PET beverage bottles and PP disposable plates represent two food-contact applications of these polymers. Their distinct surface chemistries provide a basis for comparing how product-derived particles interact with amino acids and other biomolecules in aqueous samples. Particle association may alter the distribution of an analyte between the particulate and aqueous phases. Soluble constituents released from commercial materials and fine particles remaining after sample processing may also affect optical or enzymatic assays. The measured response can therefore reflect both analyte partitioning and matrix-dependent assay effects (Ivleva, 2021; Petersen et al., 2022; Kilincer et al., 2023, 2025; Zhang et al., 2025).

Polymer-lined paper cups provide a cellulose-rich food-contact comparator with a distinct potential source of dissolved constituents. Ranjan et al. (Ranjan et al., 2021) reported the release of dissolved ions into hot water following contact with lined paper cups. In a separate survey of polyethylene- and polystyrene-based beverage cups sold in Türkiye, Kıralan et al. (Kıralan et al., 2026) identified phthalates, bisphenol A, and several photoinitiators as potential migrants. These findings support including a commercial paper-cup material when assessing whether constituents released from food-contact products could affect an enzymatic colorimetric assay. The composition of any substances released from the cup-derived particles under the buffered conditions used here remains undetermined.

PET and PP particles have been identified in air samples and in canned sardines and sprats (Cortés-Corrales et al., 2026; Karami et al., 2018). Both polymers have also been identified in human lung tissue, and PET has been detected in human blood (Jenner et al., 2022; Leslie et al., 2022). Cellulosic fibres have been reported in indoor air and human lung tissue, although their product sources remain unknown (Dris et al., 2017; Pauly et al., 1998). These occurrence data provide context for selecting the three product-derived materials to investigate possible effects on the colorimetric determination of Phe in buffered solutions.

Commercial food-contact materials can release dissolved constituents into aqueous media. In PET bottle experiments, temperature and carbonation influenced the release of acetaldehyde, formaldehyde, and antimony into water (Bach et al., 2013). High-resolution mass spectrometry studies also documented product-dependent chemical migration from commercial plastics into water, including compounds associated with clarifying agents and coatings in reusable PP bottles (Zimmermann et al., 2021; Tisler et al., 2024). For polymer-lined paper cups, dissolved ions were detected in hot water after contact (Ranjan et al., 2021). Phthalates, bisphenol A, and photoinitiators have also been identified as potential migrants in commercial beverage-cup samples (Kıralan et al., 2026). Together, these studies show that the chemical composition of an aqueous sample can change during contact with food-contact materials, with the extent and profile of release depending on the product and contact conditions.

Plastic-derived leachables can also interfere with analytical measurements. McDonald et al. (McDonald et al., 2008) demonstrated that compounds released from disposable laboratory plasticware could inhibit enzyme activity, and Lewis et al. (Lewis et al., 2010) showed that substances leached from plastic tubes contributed UV absorbance and interfered with spectrophotometric measurements of nucleic acids and proteins. In an enzyme-coupled colorimetric assay, a dissolved constituent could contribute to the optical background or alter the Phe-dependent response by affecting enzyme activity or color development. A material blank can account for an additive background signal, while a change in the response to Phe may persist after blank correction. In the present study, such effects are considered possible contributors to changes in apparent Phe signal recovery at 450 nm. The identities of any constituents released into Tris–HCl buffer and their effects on this assay remain undetermined.

A practical scenario motivating this study is the analysis of an aqueous food extract or beverage containing free phenylalanine (Phe) and particles that may be introduced during contact with packaging or tableware. PET and PP particles have been identified in canned fish, and particle release from polymer-lined paper cups has been observed during hot-water contact (Karami et al., 2018; Ranjan et al., 2021). To model the coexistence of dissolved Phe and product-derived particles, we brought ground PET, PP, and paper-cup materials into contact with buffered Phe solutions. This controlled system allowed us to compare changes in the enzymatic colorimetric response under defined conditions. The applicability of these effects to food extracts, beverages, and clinical specimens remains to be established.

An important distinction is that environmental sorption experiments and analytical interference experiments interrogate overlapping but nonidentical phenomena. A lower concentration in the recovered aqueous fraction may arise from binding to particle surfaces, retention during filtration, or transformation of the analyte. However, suppression of a post-filtration enzymatic color signal can also reflect interference by filter-passing material or extractable matrix constituents. Without an independent reference measurement, these pathways cannot be assigned quantitatively from absorbance changes alone. This concern is especially relevant when a colorimetric assay is used to infer depletion following prolonged contact with heterogeneous particulate materials (Ivleva, 2021; Petersen et al., 2022; Kilincer et al., 2023; Zhang et al., 2025; Kilincer et al., 2025).

To address this question, the present study assessed changes in the enzymatic colorimetric Phe readout after contact with particles prepared from a commercial PET bottle and PP plate and with a cellulose-rich material obtained from a paper cup, used here as a non-plastic particulate comparator. Three nominal particle loadings (1, 3, and 10 mg/mL), three initial Phe concentrations (20, 60, and 100 µm; equivalent to nominal assay-well concentrations of approximately 17, 50, and 83 µm), and five contact durations (nominally 2, 6, 24, 48, and 96 h) were investigated. After filtration, the recovered aqueous fractions were analyzed through an

https://doi.org/10.25135/jcm.2610-4051
J. Chem. Metrol. 2026, 20(2):e26104051

Table 1. Characteristics of the commercial materials used for particle preparation

Source material	Predominant component	Color
Plastic water bottle	Polyethylene terephthalate (PET)	Blue
Disposable plastic plate	Polypropylene (PP)	White
Paper cup	Cellulose-based material (CEL)	White

enzyme/developer-based assay at 450 nm. Rather than treating every decline in signal as adsorption, we define the primary outcome as apparent analytical signal recovery relative to time- and concentration-matched Phe-only controls. The study thereby tests the extent to which material identity, loading, analyte level, and duration influence apparent Phe determination and identifies the controls needed to differentiate analyte partitioning from assay-specific interference.

2 Materials and Methods

2.1 Materials and Reagents

A commercial phenylalanine (Phe) colorimetric assay kit containing phenylalanine assay buffer, enzyme mix, and phenylalanine developer was obtained from Abcam. L-Phenylalanine, tris(hydroxymethyl)aminomethane (Tris), and hydrochloric acid (HCl) were used for the preparation of standard solutions and reaction media. Ultrapure water was obtained using a Milli-Q purification system (Millipore, USA).

Three commercially available consumer products, including polyethylene terephthalate (PET) water bottles, polypropylene (PP) disposable plates, and cellulose-based paper cups, were purchased from local markets. These materials were selected to investigate the influence of particulate material composition on the analytical determination of Phe. The characteristics of the selected materials are summarized in Table 1.

2.2 Preparation and Spectroscopic Characterization of Particulate Materials

PET, PP, and cellulose-based particles were prepared by mechanical fragmentation of the corresponding commercial materials. Before fragmentation, the materials were thoroughly washed with ultrapure water and dried at room temperature. The dried materials were mechanically ground using a stainless-steel grater and subsequently sieved to obtain particulate fractions suitable for the experimental procedures. The resulting particles were washed again with ultrapure water and allowed to dry at room temperature before use.

The chemical composition of the prepared particulate materials was examined using Fourier-transform infrared (FTIR) and Raman spectroscopy. FTIR measurements were performed over the spectral range of 400–4000 cm^{-1} to identify characteristic functional groups and confirm the predominant chemical composition of the materials. Raman spectroscopy was additionally employed to examine characteristic molecular vibrations associated with the polymeric and cellulose-based structures.

The spectral characteristics were evaluated based on the positions and assignments of the principal vibrational bands. These analyses provided chemical identification of the prepared materials and a basis for discussing potential material-dependent interactions with Phe.

2.3 Preparation of Phenylalanine Standards and Enzymatic Colorimetric Assay

A 50 mM Tris–HCl buffer (pH 8.5) was prepared by dissolving 1.51 g of Tris in ultrapure water, adjusting the pH to 8.5 using 0.1 M HCl, and diluting to a final volume of 250 mL.

A 10 mM Phe stock solution was prepared by dissolving 16.5 mg of L-phenylalanine in ultrapure water and adjusting the final volume to 10 mL. A 1 mM working solution was subsequently prepared by diluting 2.5 mL of the 10 mM stock solution to 25 mL with 50 mM Tris–HCl buffer.

The enzymatic colorimetric assay was performed using a modified microplate-based procedure. Calibration standards were prepared by transferring 2, 4, 6, 8, and 10 µL of the 1 mM Phe working solution into individual microplate wells and adjusting the volume to 100 µL with Tris–HCl buffer. These solutions corresponded to initial Phe concentrations of 20, 40, 60, 80, and 100 µm, respectively.

A 20 µL reaction mixture containing 19.2 µL of Tris–HCl buffer, 0.4 µL of enzyme mix, and 0.4 µL of phenylalanine developer was subsequently added to each well. The final reaction volume was 120 µL, resulting in nominal Phe concentrations of approximately 17, 33, 50, 67, and 83 µm.

The reaction mixtures were mixed for 3 min and incubated at 37°C for 30 min. Following incubation, absorbance was measured at 450 nm using a UV–Vis spectrophotometric microplate measurement system.

Reagent blanks were prepared using Tris–HCl buffer without Phe and processed under the same incubation and measurement conditions. The analytical response was evaluated using blank-corrected absorbance values at 450 nm (A_{450}). Calibration curves were constructed by plotting A_{450} against the nominal final Phe concentrations.

The linear calibration relationship was determined by least-squares regression. The limits of detection (LOD) and quantification (LOQ) were calculated according to:

LOD = 3s/b

LOQ = 10s/b

where (b) represents the slope of the calibration curve and (s) represents the standard deviation estimate used for the analytical response.

2.4 Experimental Design for Evaluating Particulate Interference in Phenylalanine Determination

The influence of particulate material contact on the enzymatic colorimetric determination of Phe was investigated using PET, PP, and cellulose-based particles at three particle loadings, three Phe concentrations, and five contact durations.

For each experimental condition, 1, 3, or 10 mg of the prepared particulate material was transferred into an individual microcentrifuge tube. Subsequently, 20, 60, or 100 µL of the 1 mM Phe working solution was added, and the total volume was adjusted to 1 mL using 50 mM Tris–HCl buffer (pH 8.5). The resulting suspensions contained particle concentrations of 1, 3, or 10 mg/mL and initial Phe concentrations of 20, 60, or 100 µm.

Ground PET, PP, and cellulose-rich paper-cup material were added to buffered Phe solutions at nominal loadings of 1, 3, and 10 mg/mL. Loading was defined as the mass of solid material added per unit volume of the initial suspension before filtration. The same three loadings were used for each material to assess whether apparent Phe signal recovery varied with the mass of added solids across a tenfold range under otherwise identical conditions. Mixtures were maintained at room temperature for 2, 6, 24, 48, or 96 h. The 2 and 6 h time points captured changes within the first several hours of contact, and the 24, 48, and 96 h time points assessed whether the response persisted or changed over several days. At each time point, the corresponding suspensions were passed through a membrane filter with a nominal pore size of 0.45 µm to remove the bulk particulate fraction before the colorimetric assay. The loadings and contact times were selected for a controlled comparison of the three materials in buffer.

An aliquot of 100 µL of each filtrate was transferred into a microplate well, followed by the addition of 20 µL of the enzymatic reaction mixture containing 19.2 µL of Tris–HCl buffer, 0.4 µL of enzyme mix, and 0.4 µL of phenylalanine developer.

The final assay volume was 120 µL, corresponding to nominal Phe concentrations of approximately 17, 50, and 83 µm before accounting for any changes associated with particulate contact and sample processing. The reaction mixtures were mixed for 3 min and incubated at 37°C for 30 min. Absorbance was subsequently measured at 450 nm.

Phe-only control solutions were prepared without particulate material at the corresponding Phe concentrations and evaluated at the same contact durations. Particle-containing blanks without added Phe were also prepared to assess background contributions associated with the materials and sample-processing procedure. The experimental design comprised 135 particle-contact conditions, representing three materials, three particle loadings, three Phe concentrations, and five contact durations.

2.5 Evaluation of Apparent Phenylalanine Signal Recovery and Analytical Interference

The effects of particulate contact on the analytical determination of Phe were evaluated by comparing the absorbance responses of particle-contacted filtrates with those of the corresponding Phe-only controls.

Apparent signal recovery was calculated as:

$$\text{Apparent recovery (\%)} = (A_{450}, \text{sample}/A_{450}, \text{control}) \times 100$$

where (A_{450}, sample) represents the blank-corrected absorbance of the particle-contacted filtrate and (A_{450}, control) represents the blank-corrected absorbance of the corresponding Phe-only control at the same nominal Phe concentration and contact duration.

The percentage of apparent signal suppression was calculated as:

$$\text{Signal suppression (\%)} = 100 - \text{Apparent recovery (\%)}$$

An apparent recovery of 100% indicated an analytical response equivalent to that of the corresponding Phe-only control, whereas values below 100% indicated attenuation of the Phe-associated colorimetric signal following particulate contact and sample processing. Because the measurements were performed on filtered samples, the calculated recoveries represented the retained assay-detectable Phe-associated response rather than direct measurements of Phe sorption. Accordingly, the effects were interpreted as apparent analytical signal changes potentially associated with analyte partitioning, filtration-related losses, and matrix-dependent interference with the enzymatic detection reaction.

Figure 1 summarizes the experimental workflow, from particle preparation and contact with buffered phenylalanine solutions to filtration, enzymatic colorimetric measurement at 450 nm, and calculation of apparent signal recovery.

To assess the effect of filtration alone, absorbance at 450 nm was compared between filtered and unfiltered Phe solutions prepared in water without added particles. In a separate experiment, a single 20 µm Phe addition was tested after filtration under two selected contact conditions per material. The filtrates were obtained from experiments conducted either without Phe or with an initial Phe concentration of 60 µm during particle contact. For each condition, ΔA_{450} was calculated as the mean absorbance with the addition minus the mean absorbance without the addition. Each mean was based on three absorbance readings.

2.6 Data Processing and Statistical Analysis

Experimental data were processed using Microsoft Excel and Python. Calibration relationships were evaluated by linear regression, and changes in the analytical response were expressed as apparent signal recovery and signal suppression relative to the corresponding Phe-only controls.

For each particulate material, apparent recovery values were summarized across the investigated combinations of Phe concentration, particle loading, and contact duration. Descriptive statistics, including the mean, minimum, and maximum recovery values, were calculated to characterize material-dependent differences in the analytical response.

The influence of experimental conditions was visualized using comparative heat maps and time-dependent recovery

https://doi.org/10.25135/jcm.2610-4051
J. Chem. Metrol. 2026, 20(2):e26104051

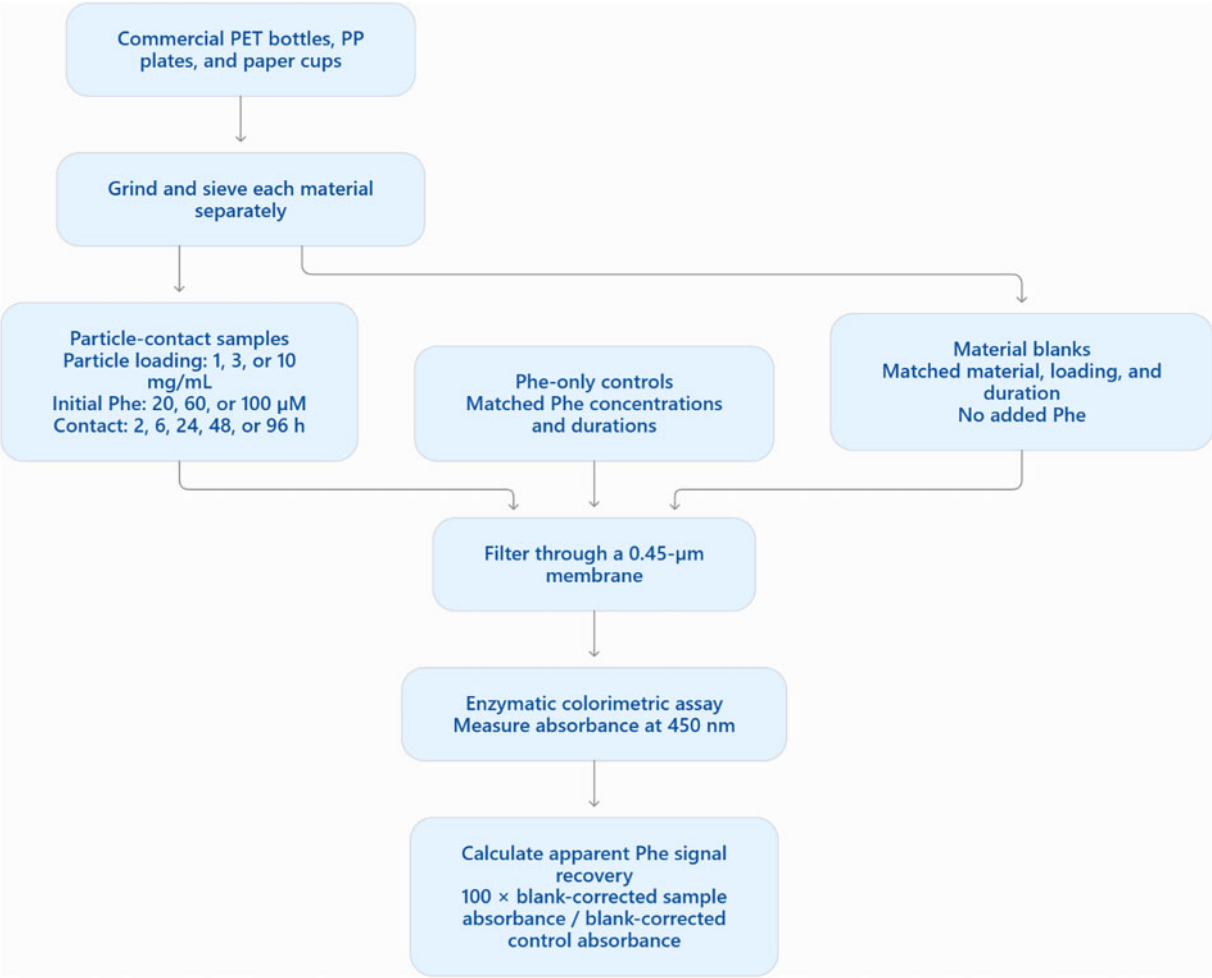

Figure 1. Experimental workflow for assessing apparent phenylalanine (Phe) signal recovery after contact with PET, PP, and cellulose-rich paper-cup particles. Each particle-contact condition was tested using three independently prepared and separately filtered samples. Initial Phe concentrations of 20, 60, and 100 µm corresponded to nominal final assay-well concentrations of approximately 17, 50, and 83 µm, respectively. Apparent signal recovery was calculated relative to the concentration- and time-matched Phe-only control using blank-corrected absorbance at 450 nm

profiles. Each particulate material was evaluated across 45 experimental conditions, comprising three Phe concentrations, three particle loadings, and five contact durations. The resulting descriptive summaries therefore represented variation across experimental conditions rather than estimates of between-replicate variability. Each condition was summarized as the mean and sample standard deviation of three independently prepared and separately filtered samples. The shared blank and matched Phe-only control were treated as fixed within each condition. The analysis was descriptive.

3 Results and Discussion

3.1 FTIR and Raman Characterization of PET, PP, and Cellulose-based Particulates

The physicochemical identity of the three commercial-source particulate materials was assessed using FTIR and Raman spectroscopy before examining their effects on Phe determination. The materials comprised mechanically fragmented PP, PET, and paper-cup samples as a cellulose-rich comparator. These distinctions are analytically important because polymer backbone chemistry and the presence of polar surface functionalities can modify wettability, interfacial contact with Phe, and the composition of the filtrate presented to the enzyme-based assay. The spectra support material assignment (Figure S1A–F).

Plate-derived particles were identified as PP based on predominantly aliphatic spectral features. FTIR bands near 972, 1019, 1374, 1420, and 2900–2969 cm^{-1} were consistent with C–H, CH_2/CH_3, and polymer backbone vibrations (Table 2). Raman features around 806–846, 976, 1086–1152, and 1332–1361 cm^{-1} further supported a PP-rich composition, consistent with published PP FTIR and Raman fingerprints (Hiejima et al., 2017; Amin et al., 2026). The hydrocarbon character of PP may favor nonpolar contacts with the aromatic side chain of Phe, although the extent of

Table 2. Representative FTIR and Raman bands used to characterize the particulate materials

Source	FTIR bands (cm^{-1})	Raman bands (cm^{-1})	Interpretation
PP plate	972, 1019, 1374, 1420; 2900–2969	806–846, 976, 1086–1152, 1332–1361	Aliphatic PP fingerprint
PET bottle	1715, 1242, 1095–1015	1616, 1732; 628, 710, 1093, 1124, 1294	Ester carbonyl/C–O and aromatic PET fingerprint
Paper cup	~3200, 2917, ~1020	907, 1099, 1123, 1386, 2923	Cellulose-rich/hydroxyl-associated fingerprint

any surface association cannot be inferred from the colorimetric response.

Bottle-derived particles showed spectral features characteristic of PET, including an FTIR band near 1715 cm^{-1} in the ester carbonyl region, bands near 1242 and 1015–1095 cm^{-1} associated with ester/C–O vibrations, and aromatic-ring-associated fingerprint features. Raman bands near 1616 and 1732 cm^{-1}, together with features around 628, 710, 1093, 1124, and 1294 cm^{-1}, were consistent with an aromatic polyester, in agreement with reported PET FTIR and Raman features (González-Córdova et al., 2023; Amin et al., 2026). PET contains ester functionalities absent from PP, providing a chemically distinct interface for contact with aqueous Phe; the spectroscopic identification does not, however, establish a specific binding mechanism.

The paper-cup-derived material exhibited cellulose-associated features, including a broad FTIR O–H region around 3200 cm^{-1}, C–H stretching near 2917 cm^{-1}, and a pronounced C–O-region band near 1020 cm^{-1}. Raman bands near 907, 1099, 1123, 1386, and 2923 cm^{-1} were compatible with a cellulose-rich composition, with bands in the O–H, C–O, and glycosidic-vibration regions consistent with reported cellulose spectra (Xu et al., 2021; Refaat et al., 2023). Because commercial paper cups may incorporate a thin polymer coating and other constituents (Xu et al., 2021), this material was treated as a cellulose-based particulate comparator rather than a chemically pure cellulose reference.

Together, the spectral results distinguish the nonpolar PP, ester-containing PET, and hydroxyl-rich cup-derived material (Figure S1; Table 2). These compositional differences provide a plausible basis for material-dependent interactions during aqueous contact and filtration. Direct confirmation of Phe sorption would require independent analysis of dissolved and particle-associated Phe fractions.

3.2 Analytical Performance of the Enzymatic Colorimetric Phenylalanine Assay

The modified enzymatic colorimetric assay generated Phe concentration-dependent absorbance spectra with a response maximum in the visible region and an analytical measurement wavelength of 450 nm, consistent with previously described enzymatic colorimetric approaches for Phe determination (Figure 2) (Schulze et al., 2002; De Silva et al., 2010). Five standards (17, 33, 50, 67, and 83 µm nominal final well concentrations) gave a linear calibration relationship, A_{450} = 0.0024 C(Phe) + 0.0124, with a correlation coefficient of r = 0.9989 (Figure 3). The calculated detection and quantification limits were 3.207 and 10.690 µm, respectively, using the 3s/b and 10s/b criteria. These parameters describe the calibration response under the assay conditions and do not by themselves establish matrix-specific analytical accuracy.

Between-day precision of the blank-corrected absorbance response at 450 nm was evaluated separately at nominal final Phe concentrations of 17, 50, and 83 µm in the assay wells. Three readings were recorded at each concentration on each of eight days. The three readings were averaged within each day, and the relative standard deviation (RSD) was calculated across the eight daily means. The between-day RSDs were 2.98% at 17 µm, 0.60% at 50 µm, and 0.21% at 83 µm. The lowest concentration showed the greatest relative variability. These values describe the between-day precision of the Phe response in Tris–HCl buffer at the three tested concentrations.

The concentration-dependent calibration response supported the use of A_{450} as an operational measure of assay-detectable Phe under the specified buffer conditions. However, the particle-contacted samples were assayed after filtration, and differences in the processed sample matrix could influence the enzyme/developer reaction (Petersen et al., 2022). Accordingly, subsequent results are expressed as apparent analytical signal recovery relative to matched Phe-only controls rather than independently validated aqueous Phe concentrations.

3.3 Material-Dependent Attenuation of the Phe-Associated Analytical Signal

The effects of particulate material contact on phenylalanine (Phe) determination were evaluated by comparing the absorbance responses of PET-, PP-, and cellulose-exposed samples with their corresponding Phe-only controls. Apparent signal recovery was calculated as the ratio of absorbance at 450 nm (A_{450}) in the particle-contacted filtrate to that of the matched Phe-only control, expressed as a percentage. Signal suppression was calculated as 100% minus apparent recovery. These parameters characterize changes in the analytical response following particulate contact.

Distinct material-associated patterns were observed across the investigated Phe concentrations, particle loadings, and contact durations (Figure 4). PET exhibited the highest overall signal retention, with a mean apparent recovery of 70.5% and individual values ranging from 40.3% to 91.2%. The corresponding mean signal suppression was 29.5%. PP produced greater attenuation, with a mean apparent recovery

https://doi.org/10.25135/jcm.2610-4051
J. Chem. Metrol. 2026, 20(2):e26104051

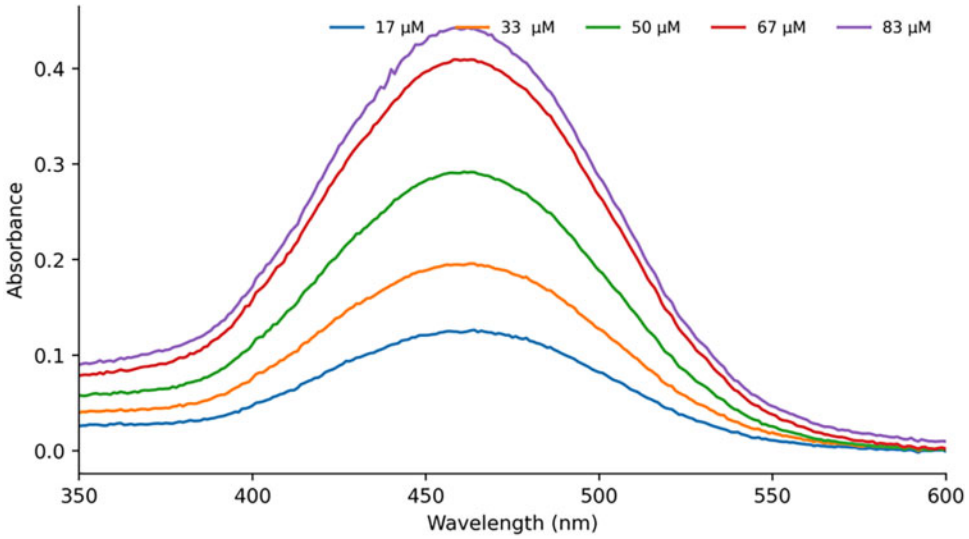

Figure 2. UV–Vis absorption spectra obtained from the enzyme/developer reaction with Phe calibration standards (17, 33, 50, 67, and 83 µm nominal final well concentrations). The analytical wavelength was 450 nm

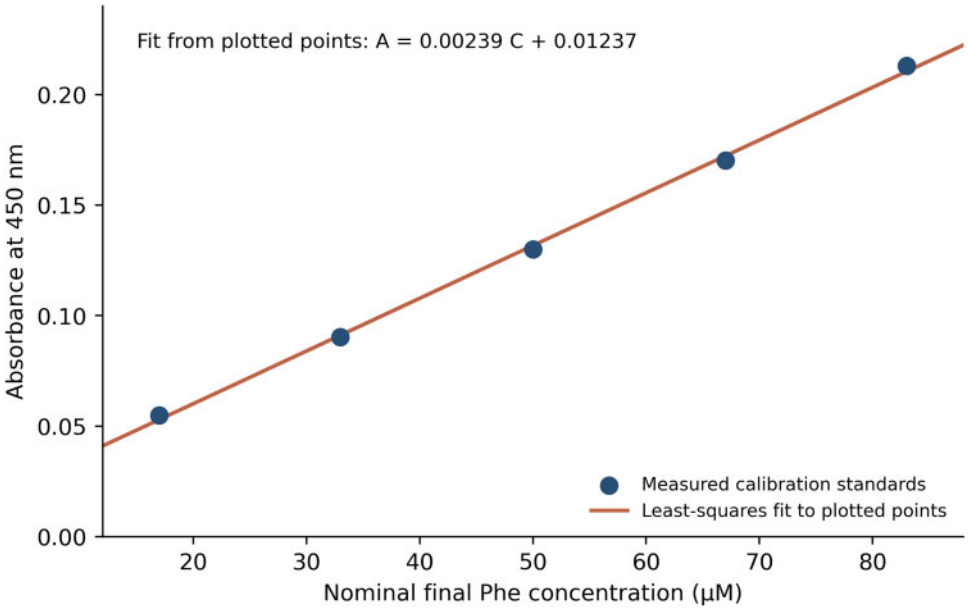

Figure 3. Calibration of the enzymatic colorimetric Phe assay at 450 nm over nominal final well concentrations of 17–83 µm. Points represent blank-corrected absorbance measurements; the line indicates least-squares linear regression

of 41.9% (range: 7.1–85.9%) and mean signal suppression of 58.1%. The cellulose-based particulate material showed the lowest overall response, with a mean apparent recovery of 7.3% (range: 0.2–24.6%) and mean signal suppression of 92.7%. Apparent signal recovery was determined from three independently prepared and separately filtered samples per condition (n = 3). Within-condition precision was expressed as the relative standard deviation (RSD), calculated as 100 × SD/mean (Cantwell, 2025). The condition-specific means, SDs, and RSDs are reported in Table S1. The RSDs ranged from 0.07% to 6.22% for PET, from 0.09% to 8.93% for PP, and from 0.37% to 11.53% for the cellulose-rich paper-cup material. For the cup-derived material, several mean recoveries were close to zero, so even a small SD could yield an appreciable RSD. The SD in percentage points therefore provides useful context for interpreting precision at low recoveries. For PP, the RSDs quantify variation among replicate samples within each condition, while Figure 4 shows how mean recovery varied across contact times, particle loadings, and Phe concentrations. The precision estimates are conditional on the shared blank and matched Phe-only control values used in the calculations.

Overall, the descriptive recovery order was PET > PP > cellulose-based particles. Previous studies report that biomolecule–microplastic interactions can vary with

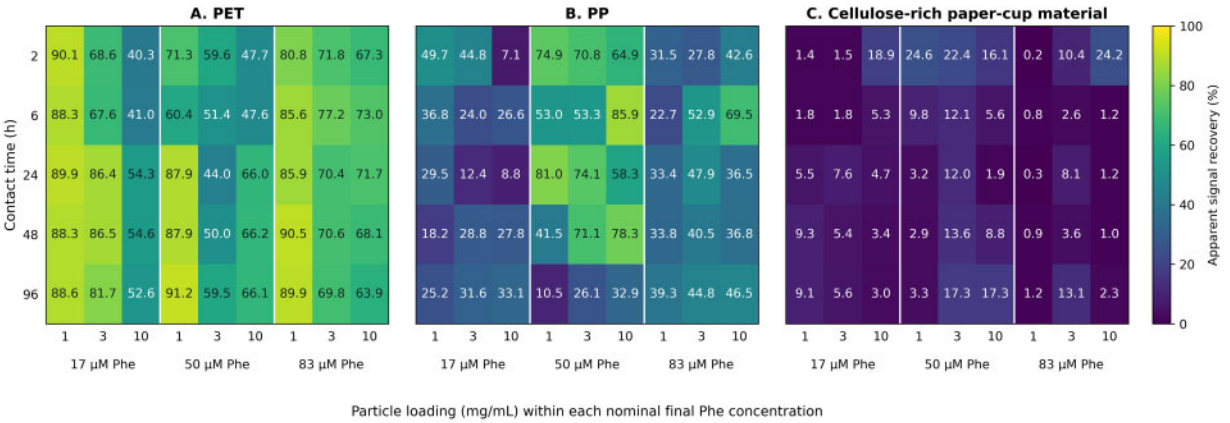

Figure 4. Multi-panel heat map of apparent Phe-associated A450 signal recovery after contact with PET, PP, and cellulose-based particles. Panels show (A) PET, (B) PP, and (C) cellulose-based comparator. Apparent recovery (%) was calculated relative to the concentration- and time-matched Phe-only control. Within each panel, columns represent combinations of nominal final Phe concentration (17, 50, and 83 µm) and particle loading (1, 3, and 10 mg/mL), while rows denote contact duration (2, 6, 24, 48, and 96 h). Each cell shows the mean apparent signal recovery from three independently prepared and separately filtered samples, rounded to one decimal place (Table S1)

both the sorbate and particle material, making particle-associated loss a plausible contributor to the observed pattern (Kilincer et al., 2023; Kilincer et al., 2025; Zhang et al., 2025). However, because A_{450} was measured in the filtrate after the enzymatic reaction, these results cannot distinguish Phe association with particles or retention during filtration from effects of filter-passing components on the enzyme/developer reaction. Such particle-related analytical artifacts require dedicated controls and independent analyte measurements to resolve (Ivleva, 2021; Petersen et al., 2022).

The low response for the paper-cup-derived material should also be interpreted in view of its commercial origin: the particulate material may contain coatings or other constituents in addition to cellulose (Xu et al., 2021). Thus, the observed recovery cannot be attributed to cellulose alone. Finally, the reported means summarize the tested conditions and are descriptive; they do not by themselves establish statistical differences among materials. Independent measurement of Phe in both the filtrate and particle-associated fractions, together with matrix-matched spike-recovery controls, would be needed to determine the contributions of analyte partitioning, filtration, and assay interference.

3.4 Dependence on Particle Loading, Phenylalanine Level, and Contact Duration

Figures 5–7 show apparent Phe signal recovery over time for PET, PP, and cellulose-rich paper-cup particles at each nominal assay-well Phe concentration. Each point represents the mean of three independently prepared and separately filtered samples (n = 3), and error bars show ±1 standard deviation (SD). Mean recoveries are expressed as percentages and SDs as percentage points. The condition-specific results are reported in Table S1.

PET contact produced distinct recovery profiles across Phe concentrations and particle loadings (Figure 5). At 17 µm Phe, the mean recovery at 1 mg/mL remained between 88.26% and 90.13% across all contact times. At 3 mg/mL, recovery increased from 68.61 ± 1.16% at 2 h to 86.53 ± 0.62% at 48 h, then decreased to 81.65 ± 0.43% at 96 h. At 10 mg/mL, recovery increased from 40.28 ± 0.51% at 2 h to 54.34 ± 1.42% at 24 h and remained between 52.61% and 54.59% thereafter. At 50 µm Phe, recovery at 1 mg/mL decreased from 71.28 ± 0.12% at 2 h to 60.35 ± 0.12% at 6 h before rising to 91.19 ± 0.06% at 96 h. At 3 mg/mL, it reached a minimum of 44.05 ± 0.12% at 24 h and rose to 59.45 ± 0.09% at 96 h. At 10 mg/mL, it increased from 47.57 ± 0.56% at 6 h to 66.01 ± 0.06% at 24 h and remained close to 66% through 96 h. At 83 µm Phe, mean recoveries across contact times ranged from 80.78% to 90.52% at 1 mg/mL, from 69.80% to 77.21% at 3 mg/mL, and from 63.86% to 72.96% at 10 mg/mL. Across the 15 conditions at each loading, mean recovery decreased from 85.1% at 1 mg/mL to 67.7% at 3 mg/mL and 58.7% at 10 mg/mL. Material properties and solution conditions can influence the sorption of organic compounds to microplastics (Kilincer et al., 2023, 2025; Zhang et al., 2025). The PET loading trend could reflect changes in Phe partitioning, the composition of the filtrate presented to the assay, or both.

PP showed nonmonotonic recovery profiles, with the ordering of the three loadings changing across Phe concentrations and contact times (Figure 6). At 17 µm Phe and 1 mg/mL PP, recovery fell from 49.68 ± 1.34% at 2 h to 18.22 ± 0.36% at 48 h, then rose to 25.20 ± 0.45% at 96 h. At 3 and 10 mg/mL, recoveries at 24 h were 12.39 ± 0.64% and 8.75 ± 0.52%, respectively, rising to 31.59 ± 0.25% and 33.10 ± 1.89% at 96 h. At 50 µm Phe, the highest means occurred at 24 h for 1 and 3 mg/mL (81.02 ± 1.36% and 74.07 ± 0.13%, respectively) and at 6 h for 10 mg/mL (85.92 ± 0.27%). By 96 h, mean recovery had fallen below 33% at all three loadings. At 83 µm Phe, recovery at 1 mg/mL ranged from 22.69% to 39.29%, while the 3 and 10 mg/mL treatments reached their highest means at 6 h (52.89 ± 0.06% and 69.46 ± 0.34%, respectively). Across the 15 conditions at each loading, mean recoveries were 38.7%, 43.4%, and 43.7% at 1, 3, and 10 mg/mL, respectively. The differences

https://doi.org/10.25135/jcm.2610-4051
J. Chem. Metrol. 2026, 20(2):e26104051

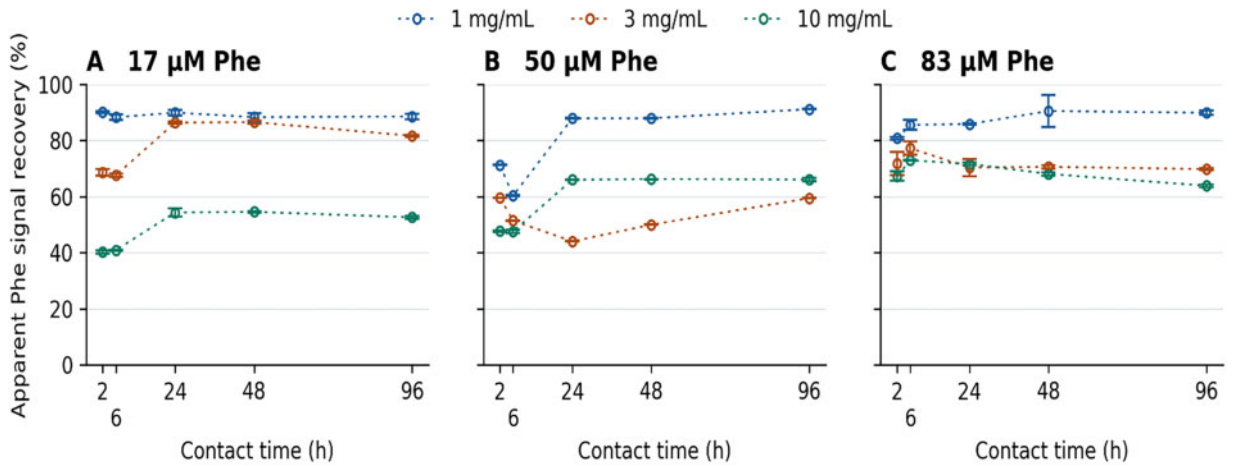

Figure 5. Time profiles of apparent Phe signal recovery after contact with PET at 1, 3, and 10 mg/mL. Panels A–C show nominal final assay-well Phe concentrations of 17, 50, and 83 µm, respectively. Recoveries were calculated relative to concentration- and time-matched Phe-only controls. Points show means from three independently prepared and separately filtered samples per condition (n = 3). Error bars indicate ±1 SD in percentage points. Dotted lines connect the means in chronological order

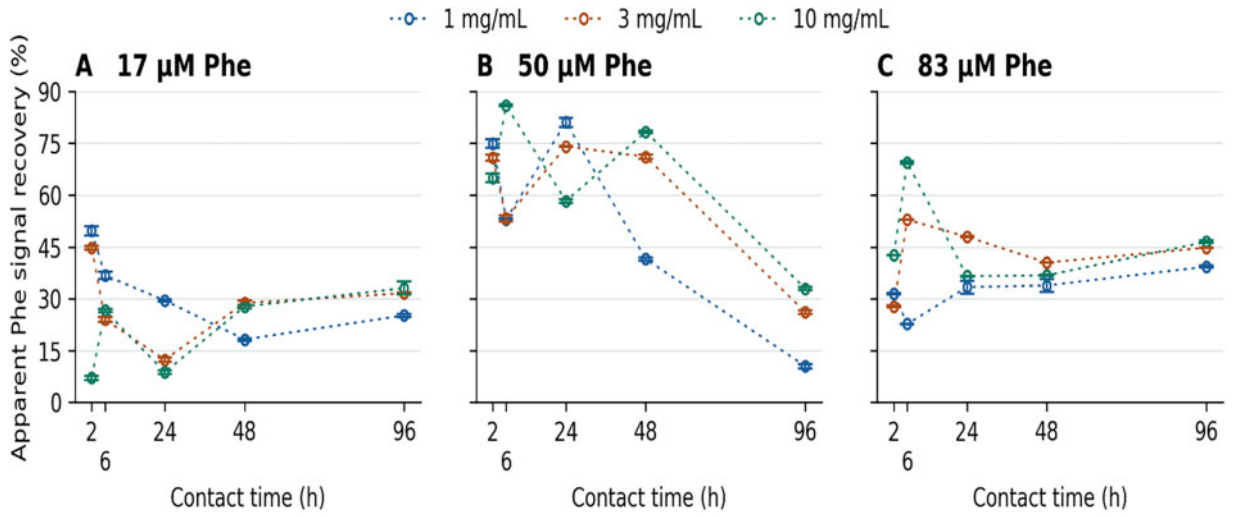

Figure 6. Time profiles of apparent Phe signal recovery after contact with PP at 1, 3, and 10 mg/mL. Panels A–C show nominal final assay-well Phe concentrations of 17, 50, and 83 µm, respectively. Recoveries were calculated relative to concentration- and time-matched Phe-only controls. Points show means from three independently prepared and separately filtered samples per condition (n = 3). Error bars indicate ±1 SD in percentage points. Dotted lines connect the means in chronological order

between selected time-point means were large relative to the corresponding within-condition SDs. Reversible association of Phe with PP and changes in the composition of the filtrate due to chemical release are possible contributors to the time profiles (Tisler et al., 2024; Xu et al., 2022).

The cellulose-rich paper-cup material generally yielded low apparent recoveries, with higher values at selected time points (Figure 7). At 17 µm Phe, mean recovery was below 10% in all conditions except at 10 mg/mL and 2 h (18.85 ± 0.70%). At that loading, recovery decreased to 5.31 ± 0.32% at 6 h and 3.04 ± 0.11% at 96 h. At 50 µm Phe and 1 mg/mL, recovery declined from 24.62 ± 0.28% at 2 h to 3.23 ± 0.33% at 24 h and remained near 3% through 96 h. At 10 mg/mL, it fell from 16.12 ± 0.83% at 2 h to 1.95 ± 0.12% at 24 h, then increased to 17.33 ± 0.16% at 96 h. At 83 µm Phe and 1 mg/mL, mean recovery ranged from 0.22% to 1.16%. At 10 mg/mL, recovery was 24.23 ± 0.26% at 2 h and ranged from 1.02% to 2.32% thereafter. At 3 mg/mL, mean recoveries reached 8.06 ± 0.20% at 24 h and 13.12 ± 0.33% at 96 h. Across the 15 conditions at each loading, mean recoveries were 5.0%, 9.1%, and 7.7% at 1, 3, and 10 mg/mL, respectively. For conditions with near-zero mean recovery, the SD in percentage points shows the absolute spread among replicates. Soluble constituents from the cup material or its coating could also affect the assay response, given that lined paper cups have been shown to release dissolved ions under hot-water contact conditions (Ranjan et al., 2021).

At the lowest nominal Phe level, the Phe-only control A_{450} was 0.0787 at 2 h, 0.0797 at 6 h, and approximately 0.101 from 24 to 96 h. Normalization to the matched control accounts

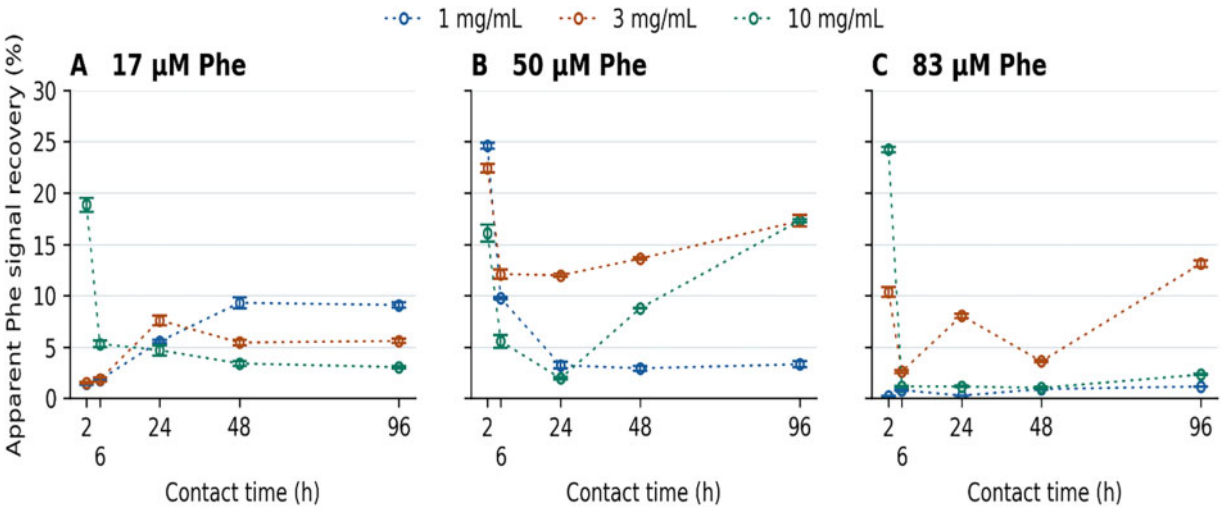

Figure 7. Time profiles of apparent Phe signal recovery after contact with cellulose-rich paper-cup particles at 1, 3, and 10 mg/mL. Panels A–C show nominal final assay-well Phe concentrations of 17, 50, and 83 µm, respectively. Recoveries were calculated relative to concentration- and time-matched Phe-only controls. Points show means from three independently prepared and separately filtered samples per condition (n = 3). Error bars indicate ±1 SD in percentage points. Dotted lines connect the means in chronological order

Table 3. Apparent Phe signal recovery and suppression across the investigated particulate-contact conditions

Material	No. of conditions	Mean recovery (%)	Min–max (%)	Mean suppression (%)
PET	45	70.5	40.3–91.2	29.5
PP	45	41.9	7.1–85.9	58.1
Cellulose-rich cup	45	7.3	0.2–24.6	92.7

for the reference response at each time point. Because the control response is the denominator, a higher control absorbance yields a lower apparent recovery for the same sample absorbance. The error bars quantify variation among the three samples at each condition with the shared blank and matched control treated as fixed. Independent measurements of dissolved and particle-associated Phe would be needed to determine how much of the observed variation reflects Phe partitioning or changes in the colorimetric response. The time profiles therefore support a descriptive comparison of apparent recovery under the tested conditions.

3.5 Distinguishing Apparent Analyte Loss from Analytical Interference

The material-dependent attenuation of the Phe colorimetric response indicates that particulate contact can alter the analytical signal even after suspended particles have been removed by filtration. Across the 45 tested conditions for each material, mean apparent recovery was highest for PET (70.5%), followed by PP (41.9%) and the cellulose-rich cup material (7.3%) (Table 3). These values describe the observed assay response; they do not establish the amount of Phe sorbed or removed from the aqueous phase. The measured A_{450} depends both on assay-detectable Phe in the filtrate and on the compatibility of that filtrate with the enzyme/developer system (Schulze et al., 2002; De Silva et al., 2010; Petersen et al., 2022).

Particle-contacted samples and their concentration- and time-matched Phe-only controls were subjected to the same 0.45-µm filtration procedure before analysis. During contact, sorption of Phe to the particles could decrease its aqueous concentration, while subsequent desorption could return particle-associated Phe to solution. Studies in related systems have documented pH-dependent sorption of thiamin onto micro- and nanoplastics (Kilincer et al., 2023) and medium-dependent desorption of previously sorbed organic compounds from microplastics (Bakir et al., 2014). These studies provide a basis for considering both processes. Their contributions under the present conditions remain unresolved because Phe concentrations in the aqueous and particle-associated fractions were not independently measured.

Leaching from the source materials could also change the composition of the solution presented to the assay. Chemical migration into water has been reported for commercial plastic products, including PET and PP bottles (Zimmermann et al., 2021; Tisler et al., 2024). Release of ions from lined paper cups has also been observed under hot-water conditions (Ranjan et al., 2021). In the present system, any dissolved constituents released during particle contact could remain in the filtrate and alter the enzyme/developer reaction or the optical response at 450 nm. Such effects could lower the measured signal at a given dissolved Phe concentration and lead to underestimation when a buffer-based calibration is

https://doi.org/10.25135/jcm.2610-4051
J. Chem. Metrol. 2026, 20(2):e26104051

applied. The results are therefore expressed as apparent signal recovery relative to matched Phe-only controls. The experiments were conducted in 50 mM Tris–HCl buffer (pH 8.5), and whether comparable effects occur in biological samples remains unknown.

PET yielded the highest mean apparent signal recovery (70.5%), with a general decrease as particle loading increased. The ester and aromatic groups identified by FTIR and Raman spectroscopy provide a chemical basis for considering polar and aromatic interactions with Phe. The loading-associated decline is consistent with a greater extent of particle contact at higher PET masses. However, increasing the PET loading could also increase the amount of material-derived constituents released into the buffer. Chemical migration from PET bottles into water has been documented in other systems (Tisler et al., 2024), and the relative contributions of Phe sorption and leachate-related assay effects remain unresolved here.

PP showed a lower mean apparent recovery (41.9%) and a nonmonotonic response across particle loadings. Given the predominantly aliphatic character of PP, hydrophobic association with the phenyl side chain of Phe is one possible pathway. Chemical migration from commercial PP products into water has also been documented (Tisler et al., 2024), providing a basis for considering effects of product-derived constituents on the colorimetric response. The time-dependent fluctuations in apparent recovery cannot be assigned to Phe desorption from the absorbance profiles alone.

The cellulose-rich, paper-cup-derived particles produced the lowest mean apparent recovery (7.3%). The hydroxyl-rich matrix provides potential sites for hydrogen bonding with Phe. Other constituents of the commercial cup material could also contribute to the response. For example, ion release from lined paper cups has been documented during hot-water contact (Ranjan et al., 2021). The extent and composition of any release under the room-temperature buffered conditions used here remain unknown. Thus, the pronounced signal suppression identifies the cup-derived material as the source of the largest change in assay response under the tested conditions, while its Phe sorption capacity remains undetermined.

The relative contributions of analyte depletion and assay-related interference could be distinguished through complementary analytical approaches. Recovery experiments involving the addition of known Phe concentrations to particle-conditioned filtrates would help establish whether soluble matrix constituents affect the enzymatic response. Filtration controls without particle exposure would allow the contribution of membrane-associated losses to be evaluated, while independent quantification using HPLC or LC–MS/MS could determine whether attenuation of the colorimetric signal corresponds to a measurable decrease in aqueous Phe concentration. Analysis of the particle-associated fraction would provide additional evidence for sorption-mediated removal.

Collectively, the material-dependent results indicate that contact and filtration can alter enzymatic Phe assay responses through processes that are not distinguishable from absorbance data alone. Matrix-matched spike recovery, filtration controls, and independent chromatographic determination of aqueous Phe would be needed to partition the contributions of analyte removal and assay-specific interference.

The filtration-only comparison showed no statistically significant difference in absorbance between filtered and unfiltered Phe solutions prepared in water under the conditions tested. In the post-filtration addition experiment, the response to 20 µm Phe varied across the selected particle-contact conditions (Table S2). For filtrates from experiments initiated with 60 µm Phe, ΔA_{450} ranged from +0.0010 to +0.0046 for PET, +0.0253 to +0.0272 for PP, and +0.0024 to +0.0153 for the cellulose-rich paper-cup material. Among filtrates prepared without Phe during particle contact, mean absorbance decreased after Phe addition for PET at 24 h (ΔA_{450} = −0.0049) and PP at 96 h (ΔA_{450} = −0.0201). These responses indicate that the colorimetric signal increment depended on the filtrate conditions and are consistent with possible matrix interference.

3.6 Exploratory FTIR Profiles after Phe Contact

Selected FTIR spectra of Phe-contacted particles were compared with the corresponding neat-material references to identify material-specific changes in their characteristic vibrational profiles (Figure 8).

The PET spectrum exhibited the expected ester and aromatic fingerprint, including the ester carbonyl band near 1715 cm^{-1}, ester-associated bands around 1240 and 1090 cm^{-1}, and additional features near 1016, 870, and 720 cm^{-1}. These characteristic features remained discernible after Phe contact. Relative to the neat reference, the selected PET traces showed lower transmittance at the carbonyl and fingerprint bands for 1 mg/mL at 48 h and 10 mg/mL at 2 h, whereas the 3 mg/mL at 6 h profile remained closer to the blank. The differences varied across the selected conditions and do not establish a monotonic loading response or a Phe-specific band (Amin et al., 2026).

The PP reference showed aliphatic C–H stretching bands in the 2950–2840 cm^{-1} region, CH_2/CH_3 deformation bands near 1455 and 1375 cm^{-1}, and fingerprint features around 1167, 997, 973, and 840 cm^{-1}. The post-contact spectra retained this pattern, with relatively small changes in the C–H stretching region. The 1 mg/mL, 48 h trace broadly overlapped the blank, whereas the 3 and 10 mg/mL, 24 h traces showed lower transmittance near 1455–1375 cm^{-1} and, more visibly, around 997–973 cm^{-1}. No additional band could be assigned clearly to Phe. These differences represent condition-specific profile variation rather than a complete loading–time trend (Amin et al., 2026).

The paper-cup-derived material showed a broad O–H envelope near 3330 cm^{-1}, C–H stretching near 2890 cm^{-1}, a water-associated band around 1640 cm^{-1}, and cellulose fingerprint features near 1428, 1160, 1105, 1055–1028, and 896 cm^{-1}, consistent with reported cellulose spectra (Refaat et al., 2023). The post-contact traces retained the main fingerprint pattern but showed higher transmittance than the neat reference across the O–H/C–H regions and most of

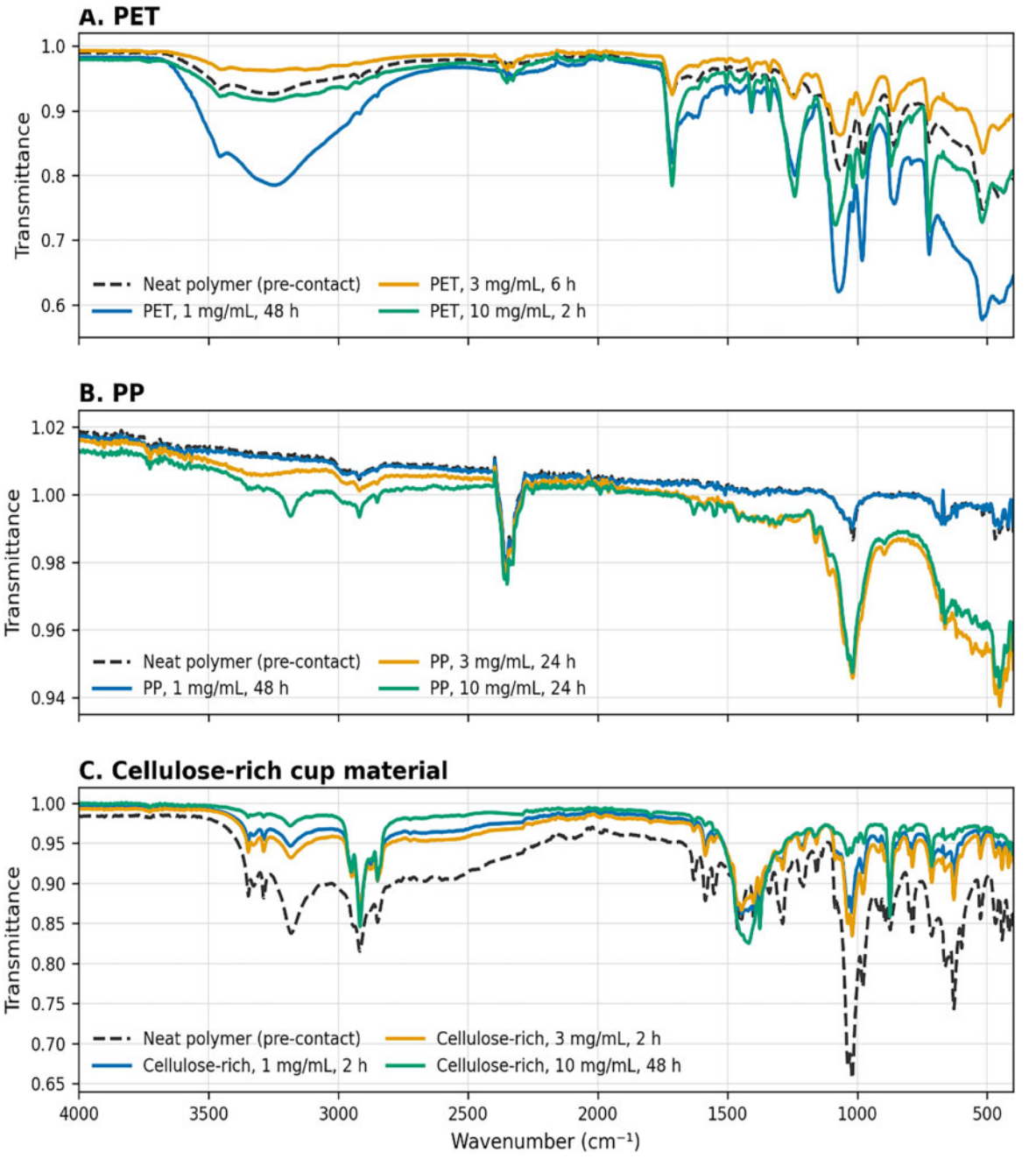

Figure 8. FTIR transmittance spectra of selected Phe-contacted particle samples compared with the corresponding neat material references measured before exposure. Dashed black traces indicate the neat, unexposed references. (A) PET at 1, 3, and 10 mg/mL after 48, 6, and 2 h, respectively; (B) PP at 1, 3, and 10 mg/mL after 48, 24, and 24 h, respectively; and (C) paper-cup-derived cellulose-rich material at 1, 3, and 10 mg/mL after 2, 2, and 48 h, respectively. Contact suspensions contained 20 μm initial Phe, equivalent to a nominal final assay-well concentration of 17 μm. Spectral differences are interpreted qualitatively.

the C–O/glycosidic fingerprint region, particularly near 1030 and 896 cm^{-1}. The 10 mg/mL, 48 h trace showed a lower-transmittance feature near 1428 cm^{-1}, illustrating that the changes were not uniform across bands.

At a given wavenumber, lower transmittance corresponds to greater apparent IR absorption by the vibrational modes in that region, whereas higher transmittance indicates weaker apparent absorption. In the selected spectra, the lower-transmittance features in PET and PP therefore indicate stronger apparent absorption at those bands. The generally higher transmittance in the cellulose-rich samples indicates weaker apparent absorption relative to the neat reference, except for the lower-transmittance feature near 1428 cm^{-1} in the 10 mg/mL, 48 h sample. These differences may reflect changes in relative band prominence or in the local sample environment. Taken together, the observed spectral changes provide a basis for considering possible material-dependent interactions between Phe and the particle surfaces. However,

https://doi.org/10.25135/jcm.2610-4051
J. Chem. Metrol. 2026, 20(2):e26104051

a uniform spectral response should not be expected because the direction and magnitude of the changes may depend on polymer composition, particle loading and available surface area, Phe concentration, and contact duration. Moreover, the FTIR comparison includes selected conditions at one initial Phe concentration rather than a complete loading–concentration–time series. The spectra therefore suggest possible Phe-associated changes but do not establish a consistent spectral trend or a specific binding mechanism. For PET, the lower transmittance near the ester carbonyl band at approximately 1715 cm^{-1} in selected Phe-contacted samples indicates greater apparent absorption in this region. The ester carbonyl oxygen could act as a hydrogen-bond acceptor for the ammonium group of Phe, and the terephthalate rings could participate in aromatic interactions with its phenyl side chain. Aromatic interactions have been proposed to contribute to the sorption of aromatic probe compounds by polystyrene (Hüffer & Hofmann, 2016), providing a precedent for considering this mechanism in an aromatic polymer. In the present PET spectra, the main difference was in apparent band intensity, and no distinct Phe-associated band could be assigned. Hydrogen bonding and aromatic association therefore remain hypotheses for the PET–Phe system.

For PP, the post-contact spectra retained the characteristic aliphatic C–H stretching and deformation bands. Given the predominantly nonpolar character of the PP backbone, the phenyl side chain of Phe could associate with the surface through hydrophobic and dispersion interactions. Sorption and desorption of phenanthrene and 1-nitronaphthalene have been examined using PP microplastics with different surface polarities (Xu et al., 2022). The PP spectra obtained here mainly showed transmittance differences in regions already assigned to the polymer. These differences provide limited molecular evidence for hydrophobic association, and the nonmonotonic apparent recovery profiles cannot establish Phe desorption.

For the cellulose-rich paper-cup material, the broad O–H band near 3330 cm^{-1} and the C–O fingerprint bands indicate a hydroxyl-rich matrix (Refaat et al., 2023). Cellulose hydroxyl groups could participate in hydrogen bonding with the ammonium and carboxylate groups of Phe. Adsorption of glycine, alanine, and proline has been reported for oxidized cellulose (Zimnitsky et al., 2005), although that material has surface carboxyl groups and differs chemically from the commercial cup material tested here. The O–H region is also sensitive to hydration, as indicated by the water-associated band near 1640 cm^{-1}. Consequently, changes in transmittance in the O–H and fingerprint regions are insufficient to assign Phe–cellulose hydrogen bonding.

The FTIR comparison covered selected particle loadings and contact times at a single initial Phe concentration (20 µm). The spectra identify functional groups that could participate in material-dependent interactions. Establishing a specific binding mechanism would require reproducible Phe-associated spectral features and independent measurements of Phe in the aqueous and particle-associated fractions.

4 Conclusion

Polymeric-particulate contact substantially attenuated the enzymatic colorimetric response used for Phe determination, with distinct patterns among PET, PP, and cellulose-based cup particles. The mean apparent signal recoveries of 70.5%, 41.9%, and 7.3%, respectively, indicate pronounced material dependence across the tested Phe concentrations, particle loadings, and contact periods. PET showed a general reduction in recovery with increasing loading, whereas PP responses were more heterogeneous; the cellulose-based comparator produced particularly low retained signals. These differences remained evident in filtrates analyzed after bulk particle removal and therefore cannot be explained solely by direct optical scattering from the original suspensions. Importantly, absorbance attenuation is not equivalent to the fraction of Phe adsorbed. The relative contributions of partitioning, filter-associated losses, and interference with enzyme/developer chemistry remain unresolved. The findings demonstrate a potential source of sample-processing and matrix-related bias in Phe colorimetric analysis under buffered conditions. The filtration-only comparison and the post-filtration Phe addition experiment helped assess potential sources of signal attenuation. Independent quantification of dissolved Phe is needed to determine how much of the attenuation arose from analyte depletion and how much from interference with the colorimetric assay.

Acknowledgement

Gülsüm Çiçek would like to thank the Institute of Graduate Studies, Istanbul University–Cerrahpaşa, for the support provided during her PhD studies entitled "Interference of Micro- and Nanoplastics in the Determination of Amino Acids and Its Mechanism". Gülsüm Çiçek would also like to express her gratitude to the Scientific and Technological Research Council of Türkiye (TÜBİTAK) for the scholarship support provided under the "TÜBİTAK 2211-A Scholarship Program" during her PhD studies between 2022 and 2026. This study was funded by Scientific Research Projects Coordination Unit of İstanbul University-Cerrahpaşa Rectorate. Project number: FDK-2024-37804.

Funding Statement

This work was supported by Scientific Research Projects Coordination Unit of Istanbul University-Cerrahpaşa Rectorate under Grant No. Project number: FDK-2024-37804.

Author Contributions

Gülsüm Çiçek: Investigation, Methodology, Validation, Formal analysis, Data curation. Hasan Saygın: Supervision, Writing—original draft, Writing—review & editing. Mustafa Özyürek: Conceptualization, Methodology, Supervision, Writing—review & editing. Aslı Baysal: Conceptualization,

Methodology, Validation, Supervision, Writing—review & editing.

Availability of Data and Materials

The authors declare that the data supporting the findings of this study are available within the paper and its Supplementary Information files. Should any raw data files be needed in another format they are available from the corresponding author upon reasonable request. Source data are provided with this paper.

Artificial Intelligence (AI) Statement

The authors utilized ChatGPT (OpenAI) for enhancing language and correcting grammatical errors. All content generated with the assistance of AI was thoroughly reviewed, verified, and sanctioned by the authors, who assume complete responsibility for the precision and integrity of the final manuscript.

Conflicts of Interest

The authors declare that they do not have any conflict of interest.

Supporting Information

Supporting information accompanies this paper on http://www.acgpubs.org/journals/journal-of-chemical-metrology.

ORCID

Gülsüm Çiçek: 0009-0008-9904-7285
Hasan Saygın: 0000-0003-2479-7635
Mustafa Özyürek: 0000-0001-5426-9775
Aslı Baysal: 0000-0002-0178-7808

References

Amin, M. L., Dinh, L. N. M., Rawal, A., Zetterlund, P. B. & Agarwal, V. (2026). Plastics recycling: A comparative study of different analytical techniques. *Macromolecular Materials and Engineering*, *311*(1), e00195. DOI: 10.1002/mame.202500195.

Bach, C., Dauchy, X., Severin, I., Munoz, J. F., Etienne, S. & Chagnon, M. C. (2013). Effect of temperature on the release of intentionally and non-intentionally added substances from polyethylene terephthalate (PET) bottles into water: Chemical analysis and potential toxicity. *Food Chemistry*, *139*(1–4), 672–680. DOI: 10.1016/j.foodchem.2013.01.046.

Bakir, A., Rowland, S. J. & Thompson, R. C. (2014). Enhanced desorption of persistent organic pollutants from microplastics under simulated physiological conditions. *Environmental Pollution*, *185*, 16–23. DOI: 10.1016/j.envpol.2013.10.007.

Cantwell, H. (Ed.). (2025), *Eurachem Guide: The Fitness for Purpose of Analytical Methods–A Laboratory Guide to Method Validation and Related Topics* (3rd ed.). http://www.eurachem.org.

Cortés-Corrales, L., Huang, M., Sahai, H., Alcayde, A., Wang, C., Hernando, M. D., Fernández-Alba, A. R. & Bueno, M. J. M. (2026). Airborne microplastics in Europe's largest plastic-covered semi-arid agricultural region. A pilot study. *Environment International*, *212*, 110314. DOI: 10.1016/j.envint.2026.110314.

De Silva, V., Oldham, C. D. & May, S. W. (2010). L-Phenylalanine concentration in blood of phenylketonuria patients: A modified enzyme colorimetric assay compared with amino acid analysis, tandem mass spectrometry, and HPLC methods. *Clinical Chemistry and Laboratory Medicine*, *48*(9), 1271–1279. DOI: 10.1515/CCLM.2010.271.

Dris, R., Gasperi, J., Mirande, C., Mandin, C., Guerrouache, M., Langlois, V. & Tassin, B. (2017). A first overview of textile fibers, including microplastics, in indoor and outdoor environments. *Environmental Pollution*, *221*, 453–458. DOI: 10.1016/j.envpol.2016.12.013.

González-Córdova, J. A., Ariza-Flores, D., Pérez-Huerta, J. S., Madrigal-Melchor, J., López-Miranda, A. & Ortega-Gallegos, J. (2023). Optical anisotropy Raman response of polyethylene terephthalate strained thin films. *Physica B: Condensed Matter*, *654*, 414693. DOI: 10.1016/j.physb.2023.414693.

Hiejima, Y., Takeda, K. & Nitta, K. H. (2017). Investigation of the molecular mechanisms of melting and crystallization of isotactic polypropylene by in situ Raman spectroscopy. *Macromolecules*, *50*(15), 5867–5876. DOI: 10.1021/acs.macromol.7b00229.

Hüffer, T. & Hofmann, T. (2016). Sorption of non-polar organic compounds by micro-sized plastic particles in aqueous solution. *Environmental Pollution*, *214*(17), 194–201. DOI: 10.1016/j.envpol.2016.04.018.

Ivleva, N. P. (2021). Chemical analysis of microplastics and nanoplastics: Challenges, advanced methods, and perspectives. *Chemical Reviews*, *121*(19), 11886–11936. DOI: 10.1021/acs.chemrev.1c00178.

Jenner, L. C., Rotchell, J. M., Bennett, R. T., Cowen, M., Tentzeris, V. & Sadofsky, L. R. (2022). Detection of microplastics in human lung tissue using μFTIR spectroscopy. *Science of the Total Environment*, *831*, 154907. DOI: 10.1016/j.scitotenv.2022.154907.

Karami, A., Golieskardi, A., Choo, C. K., Larat, V., Karbalaei, S. & Salamatinia, B. (2018). Microplastic and mesoplastic contamination in canned sardines and sprats. *Science of the Total Environment*, *612*, 1380–1386. DOI: 10.1016/j.scitotenv.2017.09.005.

Kilincer, M., Saygin, H., Ozyurek, M. & Baysal, A. (2023). Sorption of thiamin (vitamin B1) onto micro(nano)plastics: pH dependence and sorption models. *Journal of Environmental Science and Health, Part A*, *58*(8), 762–772. DOI: 10.1080/10934529.2023.2216123.

Kilincer, M., Saygin, H., Ozyurek, M. & Baysal, A. (2025). Impact of the in vitro human digestive environment on the interaction between vitamin C and microplastics. *Analytical Letters*, *58*(12), 2087–2102. DOI: 10.1080/00032719.2024.2368021.

Kıralan, S., Toptancı, İ. & Sezer, C. (2026). Migration of phthalates, bisphenols, photoinitiators, and perfluorinated compounds in polyethylene and polystyrene based beverage cups. *Journal of Environmental Science and Health, Part B*, *61*(4), 176–184. DOI: 10.1080/03601234.2026.2633932.

Leslie, H. A., Van Velzen, M. J., Brandsma, S. H., Vethaak, A. D., Garcia-Vallejo, J. J. & Lamoree, M. H. (2022). Discovery and quantification of plastic particle pollution in human blood. *Environment International*, *163*(2), 107199. DOI: 10.1016/j.envint.2022.107199.

Lewis, L. K., Robson, M. H., Vecherkina, Y., Ji, C. & Beall, G. W. (2010). Interference with spectrophotometric analysis of nucleic acids and proteins by leaching of chemicals from plastic tubes. *Biotechniques*, *48*(4), 297–302. DOI: 10.2144/000113387.

McDonald, G. R., Hudson, A. L., Dunn, S. M., You, H., Baker, G. B., Whittal, R. M., Martin, J. W., Jha, A., Edmondson, D. E. & Holt, A. (2008). Bioactive contaminants leach from disposable laboratory plasticware. *Science*, *322*(5903), 917. DOI: 10.1126/science.1162395.

OECD. (2022). *Global Plastics Outlook: Policy Scenarios to 2060*. Paris: OECD Publishing. DOI: 10.1787/aa1edf33-en.

Pauly, J. L., Stegmeier, S. J., Allaart, H. A., Cheney, R. T., Zhang, P. J., Mayer, A. G., & Streck, R. J. Inhaled cellulosic and plastic fibers found in human lung tissue. *Cancer Epidemiol Biomarkers Prev*, 1998;*7*(5):419–28.

Peat, J. & Garg, U. (2016). Determination of phenylalanine and tyrosine by high-performance liquid chromatography-tandem mass spectrometry. In: Garg, U. (Eds.), *Clinical applications of mass spectrometry in biomolecular analysis: Methods in Molecular Biology* (Vol. 1378). New York, NY: Humana Press. DOI: 10.1007/978-1-4939-3182-8_23.

Petersen, E. J., Barrios, A. C., Henry, T. B., Johnson, M. E., Koelmans, A. A., Montoro Bustos, A. R., Matheson, J., Roesslein, M., Zhao, J. & Xing, B. (2022). Potential artifacts and control experiments in toxicity tests of nanoplastic and microplastic particles. *Environmental Science & Technology*, *56*(22), 15192–15206. DOI: 10.1021/acs.est.2c04929.

Pinto, A., Ilgaz, F., Evans, S., van Dam, E., Rocha, J. C., Karabulut, E., Hickson, M., Daly, A. & MacDonald, A. (2023). Phenylalanine tolerance over time in phenylketonuria: A systematic review and meta-analysis. *Nutrients*, *15*(16), 3506. DOI: 10.3390/nu15163506.

PlasticsEurope. (2025). *Plastics the fast facts 2025: Global and European plastics production and economic indicators*. https://plasticseurope.org/knowledge-hub/plastics-the-fast-facts-2025/.

Ranjan, V. P., Joseph, A. & Goel, S. (2021). Microplastics and other harmful substances released from disposable paper cups into hot water. *Journal of Hazardous Materials*, *404*, 124118. DOI: 10.1016/j.jhazmat.2020.124118.

Refaat, A., Elhaes, H. & Ibrahim, M. A. (2023). Effect of alkali metals on physical and spectroscopic properties of cellulose. *Scientific Reports*, *13*, 21649. DOI: 10.1038/s41598-023-48850-7.

Rudy, J. L., Rutledge, J. C. & Lewis, S. L. (1987). Phenylalanine and tyrosine in serum and eluates from dried blood spots as determined by reversed-phase liquid chromatography. *Clinical Chemistry*, *33*(7), 1152–1154. DOI: 10.1093/clinchem/33.7.1152.

Schulze, A., Mayatepek, E. & Hoffmann, G. F. (2002). Evaluation of 6-year application of the enzymatic colorimetric phenylalanine assay in the setting of neonatal screening for phenylketonuria. *Clinica Chimica Acta*, *317*(1–2), 27–37. DOI: 10.1016/S0009-8981(01)00736-7.

Sebastião, F. M., Burin, M. G., Civallero, G., Tirelli, K. M., Sitta, A., Coelho, D. D. M., Vargas, C. R., Wajner, M., Giugliani, R., Bitencourt, F. H. & Schwartz, I. V. D. (2020). Monitoring of phenylalanine levels in patients with phenylketonuria using dried blood spots: A comparison of two methods. *Journal of Inborn Errors of Metabolism and Screening*, *8*, e20190011. DOI: 10.1590/2326-4594-JIEMS-2019-0011.

Tisler, S., Kristiansen, N. & Christensen, J. H. (2024). Chemical migration from reusable plastic bottles: Silicone, polyethylene, and polypropylene show highest hazard potential in LC-HRMS analysis. *Journal of Hazardous Materials*, *480*, 136391. DOI: 10.1016/j.jhazmat.2024.136391.

Waisbren, S. E., Noel, K., Fahrbach, K., Cella, C., Frame, D., Dorenbaum, A. & Levy, H. (2007). Phenylalanine blood levels and clinical outcomes in phenylketonuria: A systematic literature review and meta-analysis. *Molecular Genetics and Metabolism*, *92*(1–2), 63–70. DOI: 10.1016/j.ymgme.2007.05.006.

Xu, J., Zhang, K., Wang, L., Yao, Y. & Sun, H. (2022). Strong but reversible sorption on polar microplastics enhanced earthworm bioaccumulation of associated organic compounds. *Journal of Hazardous Materials*, *423*(1), 127079. DOI: 10.1016/j.jhazmat.2021.127079.

Xu, Z., Zhou, Q., Wang, L., Xia, G., Ji, X., Zhang, J., Zhang, J., Nawaz, H., Wang, J. & Peng, J. (2021). Transparent cellulose-based films prepared from used disposable paper cups via an ionic liquid. *Polymers*, *13*(23), 4209. DOI: 10.3390/polym13234209.

Zhang, T., Wang, Z., Wu, Y., Zhu, S. & Su, J. (2025). Interactions of micro- and nanoplastics with biomolecules: From public health to protein corona effect and beyond. *The Journal of Physical Chemistry B*, *129*(22), 5355–5374. DOI: 10.1021/acs.jpcb.5c00416.

Zimmermann, L., Bartosova, Z., Braun, K., Oehlmann, J., Völker, C. & Wagner, M. (2021). Plastic products leach chemicals that induce in vitro toxicity under realistic use conditions. *Environmental Science & Technology*, *55*(17), 11814–11823. DOI: 10.1021/acs.est.1c01103.s001.

Zimnitsky, D. S., Yurkshtovich, T. L. & Bychkovsky, P. M. (2005). Multilayer adsorption of amino acids on oxidized cellulose. *Journal of Colloid and Interface Science*, *285*(2), 502–508. DOI: 10.1016/j.jcis.2004.12.021.